The Journal of the Anti-Seismic Systems International Society (ASSISi)

Seismic Isolation and Protection Systems

ASSESSMENT OF PERFORMANCE DEGRADATION IN ENERGY DISSIPATORS INSTALLED ON BRIDGE STRUCTURES

Gianmario Benzoni and Carmen Amaddeo

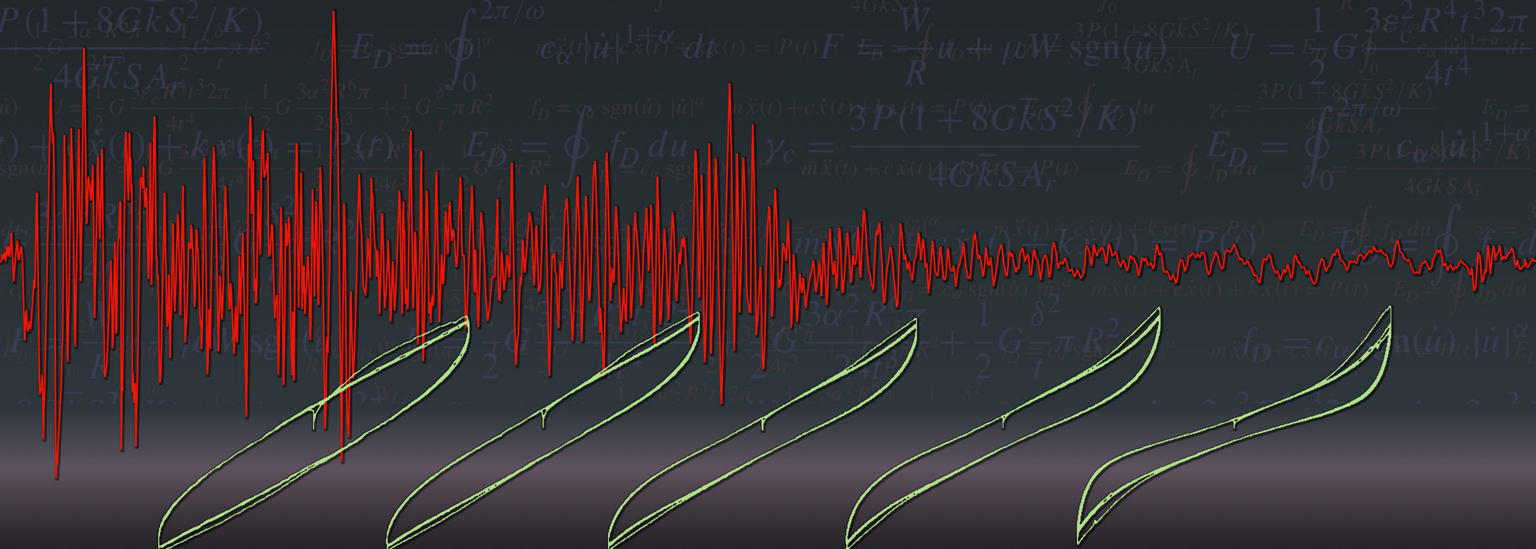

vol 1, no 1 2010

mathematical sciences publishers

mathematical sciences publishers + Anti-Seismic Systems International Society
SEISMIC ISOLATION AND PROTECTION SYSTEMS 1:1 (2010)

ASSESSMENT OF PERFORMANCE DEGRADATION IN ENERGY DISSIPATORS INSTALLED ON BRIDGE STRUCTURES

GIANMARIO BENZONI AND CARMEN AMADDEO

A health monitoring technique for estimating the performance degradation of antiseismic devices is presented. The approach was validated through data obtained from a 3D finite element model of a bridge structure as well as through records obtained from a real bridge equipped with viscous dampers. The records from the real structure were collected during ambient vibrations as well as a seismic event. The procedure appears capable of detecting early stages of performance variation in the devices, both in terms of location and severity level. It also requires a rather limited number of sensors, typical of a basic monitoring installation. The procedure appears feasible for application to many devices commonly installed in bridges.

1. Introduction

An effective health monitoring approach for the assessment of changes in the performance of energy dissipators in service is defined. The devices specifically considered in this study are viscous dampers (energy dissipators), but the proposed algorithm, and particularly the general procedure, can be adapted to structures equipped with other antiseismic devices. Variations in the performance characteristics of these protection systems have proved difficult to detect by traditional approaches that belong to the broad category of global (macro) methods. These approaches use measurements from a dispersed set of sensors to obtain global information about the condition of the entire structure [Housner et al. 1997]. The scope of monitoring the performance of bridges with seismic response modification devices (SRMDs), due to the concentration of nonlinear, large deformation behavior into one group of elements, pertains instead naturally to the category of local (micro) methods, which are designed to monitor specific components of the overall structural system. The ideal approach should provide a level of integration between global and local performance in order to allow for the assessment of the impact on the overall bridge response of the performance degradation detected at the local level. The proposed algorithm follows this approach by providing an assessment of the performance degradation of local components obtained from changes in modal characteristics of the overall structure.

The main case study in this research is the Vincent Thomas Bridge, a cable-suspension structure retrofitted in different stages, and lately equipped with 48 viscous dampers. The study was conducted by means of nonlinear time-history analyses of a detailed three-dimensional FE model of the bridge, provided by the California Department of Transportation (Caltrans), used in the validation phase of the procedure. Real acceleration records, obtained from the bridge under ambient vibrations and a seismic event, were used, in a second phase of development, to demonstrate the validity and accuracy of the procedure.

Keywords: bridge, dampers, damage assessment.

2. Definition of the damage detection algorithm

The core of the proposed algorithm consists of an existing damage detection algorithm modified and extended to the specific case of a bridge structure equipped with energy dissipators. The method can identify whether damage has occurred and can determine the location and severity of the damage. The sequence of procedural steps is summarized hereafter and is shown schematically in Figure 1.

Step 1. Two sources of records of the structural response were used. A three-dimensional finite element model of the Vincent Thomas Bridge provided acceleration records under white noise excitations. Records from ambient vibrations and a recent seismic event, obtained with the existing sensor network of the same bridge, were also analyzed. A model of a simplified frame, with applied viscous dampers, was used, in the early development phase, in order to validate the approach. The results of this initial phase are not reported here, but details can be found in [Benzoni et al. 2007]. Through the finite element model, the bridge structure was initially analyzed in an undamaged configuration and subsequently modified to artificially create localized degradation conditions in the viscous dampers, at different levels of severity. The simulated damages were introduced as a reduction of both stiffness and viscous dissipative properties of the energy dissipators. The data obtained from the sensor network available on the real bridge structure were also used and indicated, through the proposed procedure, that the viscous devices were at different

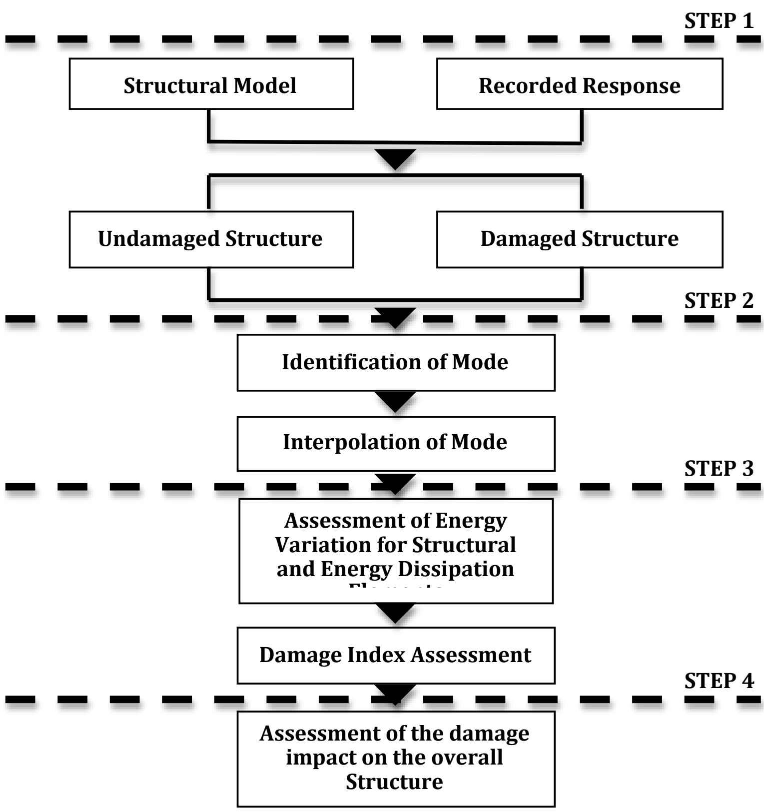

Figure 1. Layout of analytical approach.

levels of functionality. Four dampers on the bridge, in fact, suffered different degrees of damage and had to be replaced with new, identical devices. Data were recorded from the bridge with dampers in new as well as degraded conditions.

Step 2. For both the bridge model and the real structure, the natural frequencies and mode shapes of the first three significant modes were extracted. The procedure can be extended to a larger number of modes, but for the purposes of this investigation the first three modes appeared to provide sufficient information for the damage identification process. The covariance-driven stochastic subspace identification method (SSI-Cov) [Peeters 2000] was used for the assessment of the modal characteristics.

Step 3. The nondestructive damage evaluation method was applied by comparing pre-damage and post-damage configurations of the structure in terms of energy content, obtained from flexural and axial deformations. Deformations were calculated from the previously assessed mode shapes through interpolating polynomial functions. A damage index, associated with arbitrary structural elements as well as with the damping devices, was calculated.

Step 4. The structural degradation thus detected was then assigned a damage severity level.

2.1. ***Implementation of the original procedure.*** The original procedure was introduced in [Stubbs et al. 1992]. If a linear elastic beam is considered, the i-th modal stiffness is obtained as

$$K_i = \int_0^L EI(x)[\psi_i''(x)]^2 dx,$$

where L is the total length of the beam, ψ_i is the i-th mode shape and $EI(x)$ is the beam bending stiffness. Assuming the beam discretized into a number of elements and nodes, the contribution to the i-th modal stiffness of the j-th element can be expressed as

$$K_{ij} = EI_j \int_a^b [\psi_i''(x)]^2 dx,$$

where EI_j is the stiffness of the j-th element integrated along the length of the single element. The limits a and b generically indicate the boundary of the element length. For simplicity, EI_j is considered here as constant along the element.

The term F_{ij} represents the fraction of modal energy for the i-th mode that is concentrated in the j-th element. and is given by

$$F_{ij} = \frac{K_{ij}}{K_i}.$$

The same quantities for the damaged structure are indicated by asterisks:

$$F_{ij}^* = \frac{K_{ij}^*}{K_i^*}.$$

The ratio between the modal energy in the damaged and undamaged states can be expressed as

$$\frac{F_{ij}^*}{F_{ij}} = \frac{K_{ij}^*/K_i^*}{K_{ij}/K_i} = \frac{EI_j^* \int_a^b [\psi_i^{*\prime\prime}(x)]^2 dx \big/ \int_0^L EI^*(x)[\psi_i^{*\prime\prime}(x)]^2 dx}{EI_j \int_a^b [\psi_i''(x)]^2 dx \big/ \int_0^L EI(x)[\psi_i''(x)]^2 dx}. \tag{2-1}$$

The assumption that $EI(x)$ is constant over the length of the beam, for both the undamaged and damaged structure, allows us to reorganize (2-1) and define the damage localization index (DI_{ij}) for the j-th element and the i-th mode as

$$DI_j = \frac{F^*_{ij}}{F_{ij}} = \frac{\int_a^b [\psi_i^{*\prime\prime}(x)]^2 dx \big/ \int_0^L [\psi_i^{*\prime\prime}(x)]^2 dx}{\int_a^b [\psi_i^{\prime\prime}(x)]^2 dx \big/ \int_0^L [\psi_i^{\prime\prime}(x)]^2 dx}. \tag{2-2}$$

In general terms, the existence of damage is indicated, for the j-th element, by $DI_{ij} > 1$. It must be noted that the possibility of very small numbers for the denominator of (2-2), for instance obtained when the j-th member is at or near a node of the i-th mode, can result in a false prediction of damage. For this reason, in some cases, a value of unity is added to the fractions of modal energy to avoid division by zero, resulting in the following equation for the damage index:

$$DI_j = \frac{F^*_{ij}+1}{F_{ij}+1} = \frac{\left(\int_a^b [\psi_i^{*\prime\prime}(x)]^2 dx + \int_0^L [\psi_i^{*\prime\prime}(x)]^2 dx\right) \int_0^L [\psi_i^{\prime\prime}(x)]^2 dx}{\left(\int_a^b [\psi_i^{\prime\prime}(x)]^2 dx + \int_0^L [\psi_i^{\prime\prime}(x)]^2 dx\right) \int_0^L [\psi_i^{*\prime\prime}(x)]^2 dx}.$$

In the original approach, the contribution of N_{mod} different modes was taken into account as a simple sum in the definition of the damage index for the j-th element:

$$DI_j = \frac{\sum_{i=1}^{N_{\text{mod}}} \left(\int_a^b [\psi_i^{*\prime\prime}(x)]^2 dx + \int_0^L [\psi_i^{*\prime\prime}(x)]^2 dx\right) \int_0^L [\psi_i^{\prime\prime}(x)]^2 dx}{\sum_{i=1}^{N_{\text{mod}}} \left(\int_a^b [\psi_i^{\prime\prime}(x)]^2 dx + \int_0^L [\psi_i^{\prime\prime}(x)]^2 dx\right) \int_0^L [\psi_i^{*\prime\prime}(x)]^2 dx}. \tag{2-3}$$

From the damage index DI_{ij} it is possible to obtain the normalized index for the j-th element and the i-th mode as

$$z_{ij} = \frac{DI_{ij} - \mu^i_{DI_{ij}}}{\sigma^i_{DI_{ij}}},$$

where $\mu^i_{DI_{ij}}$ and $\sigma^i_{DI_{ij}}$ represent the mean and standard deviation of the damage index of all the elements for the i-th mode. As indicated above, the normalized index z_j for the j-th element, taking into account the relevant number of mode shapes, is obtained as

$$z_j = \frac{DI_j - \mu_{DI}}{\sigma_{DI}},$$

where μ_{DI} and σ_{DI} represent the mean and standard deviation of the damage index of all the elements for all the considered modes. At a 98% significance level the procedure indicates the existence of damage in the j-th element if $z_j \geq 2$. The severity of damage at a given location is obtained as

$$\alpha_j = \frac{K^*_j - K_j}{K_j} = \frac{1}{DI_j - 1}, \tag{2-4}$$

where K_j and K^*_j are the stiffness terms of the elements in the undamaged and damaged configuration, respectively. The existence of damage is indicated by $\alpha_j \leq 0$.

2.2. ***Modified approach: structure with energy dissipators.*** The procedure required initially a new formulation in order to take into account the existence of the energy dissipators. The energy contribution provided by the dampers is expressed as function of the equivalent stiffness of the damper (k_{eq}):

$$E_{\text{damp}} = k_{\text{eq}} s^2,$$

where s is the length variation of the damper in relation to the modal displacements. The equivalent stiffness is obtained as

$$k_{\text{eq}} = \frac{F_{\max}}{x_{F_{\max}}},$$

where $F_{\max}$ is the peak force and $x_{F_{\max}}$ is the damper stroke (relative displacement) corresponding to the peak force value. In the definition of the damage index the energy contributions for the structural elements and for the dampers need to be combined as homogeneous quantities. For this reason the stiffness associated to the dampers is normalized to the bending stiffness of the other structural elements:

$$k_m = \frac{k_{\text{eq}}}{EI},$$

where the index m is the number of the damper. However, this level of simplification can be removed by taking into account the energy variation of each element with its pertinent level of stiffness. From the numerical point of view, an additional requirement of normalization was needed in order to maintain a level of homogenous contribution to the total energy for both the structural elements and the energy dissipators. The amplitude of the energy dissipated by the dampers is, in fact, generally much larger than the contribution from the structural elements. Numerically, this effect tends to reduce the sensitivity of the approach to changes experienced in the structural elements when the dampers are mobilized with a significant level of stroke involved. For this reason, an additional coefficient t_{im} (for each mode i and damper m) was introduced to normalize the maximum contribution of energy in the structural elements to the maximum value of energy in the dampers:

$$t_{im} = \frac{\max_{j=1,\dots,N_{\text{el}}}\left(\int_a^b [\psi_i''(x)]^2 dx\right)}{\max(k_m s_{im}^2)},$$

where the index i indicates the mode under consideration, the index m refers to the damper, k_m is the normalized damper stiffness, and s_{im} is the m-th damper length variation for the i-th mode. The numerator represents the maximum modal stiffness of each j-th element for the i-th mode shape. The denominator is the maximum modal stiffness for each m-th damper for the i-th mode shape. The index m is also needed to take into account configurations with dampers of different length, connecting nonsymmetric elements and/or having different performance characteristics.

For the damage index, the two components, for structural elements (DI_{ij}) and dampers (DI_{im}), can be obtained, respectively, as

$$DI_{ij} = \frac{\int_a^b [\psi_i^{*\prime\prime}(x)]^2 dx + \sum_{n=1}^{N_{\text{el}}} \int_0^{L_n} [\psi_i^{*\prime\prime}(x)]^2 dx + \sum_{m=1}^{N_{\text{damp}}} t_{im} (s_{im}^*)^2}{\int_a^b [\psi_i''(x)]^2 dx + \sum_{n=1}^{N_{\text{el}}} \int_0^{L_n} [\psi_i''(x)]^2 dx + \sum_{m=1}^{N_{\text{damp}}} t_{im} (s_{im})^2} \cdot \frac{\sum_{n=1}^{N_{\text{el}}} \int_0^{L_n} [\psi_i''(x)]^2 dx + \sum_{m=1}^{N_{\text{damp}}} t_{im} (s_{im})^2}{\sum_{n=1}^{N_{\text{el}}} \int_0^{L_n} [\psi_i^{*\prime\prime}(x)]^2 dx + \sum_{m=1}^{N_{\text{damp}}} t_{im} (s_{im}^*)^2}, \tag{2-5}$$

$$DI_{im} = \frac{t_{im}(s^*_{im})^2 + \sum_{n=1}^{N_{\text{el}}} \int_0^{L_n} [\psi_i^{*\prime\prime}(x)]^2 dx + \sum_{m=1}^{N_{\text{damp}}} t_{im}(s^*_{im})^2}{t_{im}(s_{im})^2 + \sum_{n=1}^{N_{\text{el}}} \int_0^{L_n} [\psi_i^{\prime\prime}(x)]^2 dx + \sum_{m=1}^{N_{\text{damp}}} t_{im}(s_{im})^2} \cdot \frac{\sum_{n=1}^{N_{\text{el}}} \int_0^{L_n} [\psi_i^{\prime\prime}(x)]^2 dx + \sum_{m=1}^{N_{\text{damp}}} t_{im}(s_{im})^2}{\sum_{n=1}^{N_{\text{el}}} \int_0^{L_n} [\psi_i^{*\prime\prime}(x)]^2 dx + \sum_{m=1}^{N_{\text{damp}}} t_{im}(s^*_{im})^2}, \tag{2-6}$$

where N_{el} is the number of subcomponents of the structure. Subcomponents are intended here as assemblies of single portions of the structure with physical significance: columns, beams, and so on. N_{damp} is the total number of dampers. The combination of the N_{mod} different modes results in a damage index for the j-th structural element, defined as

$$DI_j = \frac{\sum_{i=1}^{N_{\text{mod}}} \Bigl(\int_a^b [\psi_i^{*\prime\prime}(x)]^2 dx \sum_{n=1}^{N_{\text{el}}} \int_0^{L_n} [\psi_i^{*\prime\prime}(x)]^2 dx + \sum_{m=1}^{N_{\text{damp}}} t_{im}(s^*_{im})^2 \Bigr)}{\sum_{i=1}^{N_{\text{mod}}} \Bigl(\int_a^b [\psi_i^{\prime\prime}(x)]^2 dx + \sum_{n=1}^{N_{\text{el}}} \int_0^{L_n} [\psi_i^{\prime\prime}(x)]^2 dx + \sum_{m=1}^{N_{\text{damp}}} t_{im}(s_{im})^2 \Bigr)} \cdot \frac{\sum_{i=1}^{N_{\text{mod}}} \Bigl(\sum_{n=1}^{N_{\text{el}}} \int_0^{L_n} [\psi_i^{\prime\prime}(x)]^2 dx + \sum_{m=1}^{N_{\text{damp}}} t_{im}(s_{im})^2 \Bigr)}{\sum_{i=1}^{N_{\text{mod}}} \Bigl(\sum_{n=1}^{N_{\text{el}}} \int_0^{L_n} [\psi_i^{*\prime\prime}(x)]^2 dx + \sum_{m=1}^{N_{\text{damp}}} t_{im}(s^*_{im})^2 \Bigr)}, \tag{2-7}$$

and in a damage index for the m-th damper, defined as

$$DI_m = \frac{\sum_{i=1}^{N_{\text{mod}}} \Bigl(t_{im}(s^*_{im})^2 + \sum_{n=1}^{N_{\text{el}}} \int_0^{L_n} [\psi_i^{*\prime\prime}(x)]^2 dx + \sum_{m=1}^{N_{\text{damp}}} t_{im}(s^*_{im})^2 \Bigr)}{\sum_{i=1}^{N_{\text{mod}}} \Bigl(t_{im}(s_{im})^2 + \sum_{n=1}^{N_{\text{el}}} \int_0^{L_n} [\psi_i^{\prime\prime}(x)]^2 dx + \sum_{m=1}^{N_{\text{damp}}} t_{im}(s_{im})^2 \Bigr)} \cdot \frac{\sum_{i=1}^{N_{\text{mod}}} \Bigl(\sum_{n=1}^{N_{\text{el}}} \int_0^{L_n} [\psi_i^{\prime\prime}(x)]^2 dx + \sum_{m=1}^{N_{\text{damp}}} t_{im}(s_{im})^2 \Bigr)}{\sum_{i=1}^{N_{\text{mod}}} \Bigl(\sum_{n=1}^{N_{\text{el}}} \int_0^{L_n} [\psi_i^{*\prime\prime}(x)]^2 dx + \sum_{m=1}^{N_{\text{damp}}} t_{im}(s^*_{im})^2 \Bigr)}. \tag{2-8}$$

As indicated in (2-3) and applied in (2-7) and (2-8), consistently with the original formulation, the contribution of the different modes is combined as a simple sum, for each structural element. However, in the original format, the combination of modal contributions introduced numerical irregularities, particularly when extended to modes beyond the second. It was also noted that, in the comparison between undamaged and damaged response signals, the variation of the natural frequencies of the significant modes seems to be a reliable indicator of the importance of the modal contribution. For this reason a modal coefficient was introduced in order to take into account the variation of the natural frequencies from undamaged to damaged configuration. This coefficient, c_i, is obtained as

$$c_i = \frac{\text{abs}(f_i^* - f_i)}{\max\bigl(\text{abs}(f_i^* - f_i)\bigr)}, \tag{2-9}$$

where f_i^* and f_i are the natural frequencies of the i-th mode for the damaged and undamaged case, respectively. The coefficient c_i is multiplied by the damage index (DI_{ij}) and allows the definition of the normalized damage index Z_{ij} and Z_j, as

$$Z_{ij} = \frac{c_i DI_{ij} - \mu(c_i DI_{ij})}{\sigma(c_i DI_{ij})}, \qquad Z_j = \frac{\sum_{i=1}^{N_{\text{mod}}} c_i DI_{ij} - \mu\Big(\sum_{i=1}^{N_{\text{mod}}} c_i DI_{ij}\Big)}{\sigma\Big(\sum_{i=1}^{N_{\text{mod}}} c_i DI_{ij}\Big)}. \tag{2-10}$$

Here DI_{ij} stands for either DI_{ij} or DI_{im} when referring to structural elements or dampers, respectively. As in the original procedure, the existence of damage in the j-th element is indicated by $Z_j \geq 2$. The damage severity index α_j is obtained as in (2-4).

3. Validation of the procedure

The proposed procedure was initially applied to a simplified portal structure with applied viscous damper elements. It was tested with positive results under a large number of simulated cases of damage in both the structural elements as well as in the dampers. Unsymmetric configurations of damper locations and performance characteristics were simulated as well. Results of these preliminary analyses are not included here, but can be found in [Benzoni et al. 2007]. The validation of the approach by use of the response of a real bridge structure was initially obtained through a 3D finite element model of the Vincent Thomas Bridge (Figure 2). It must be noted that the numerical model is utilized here only to produce accelerometric response signals associated to different levels of degradation of some bridge components.

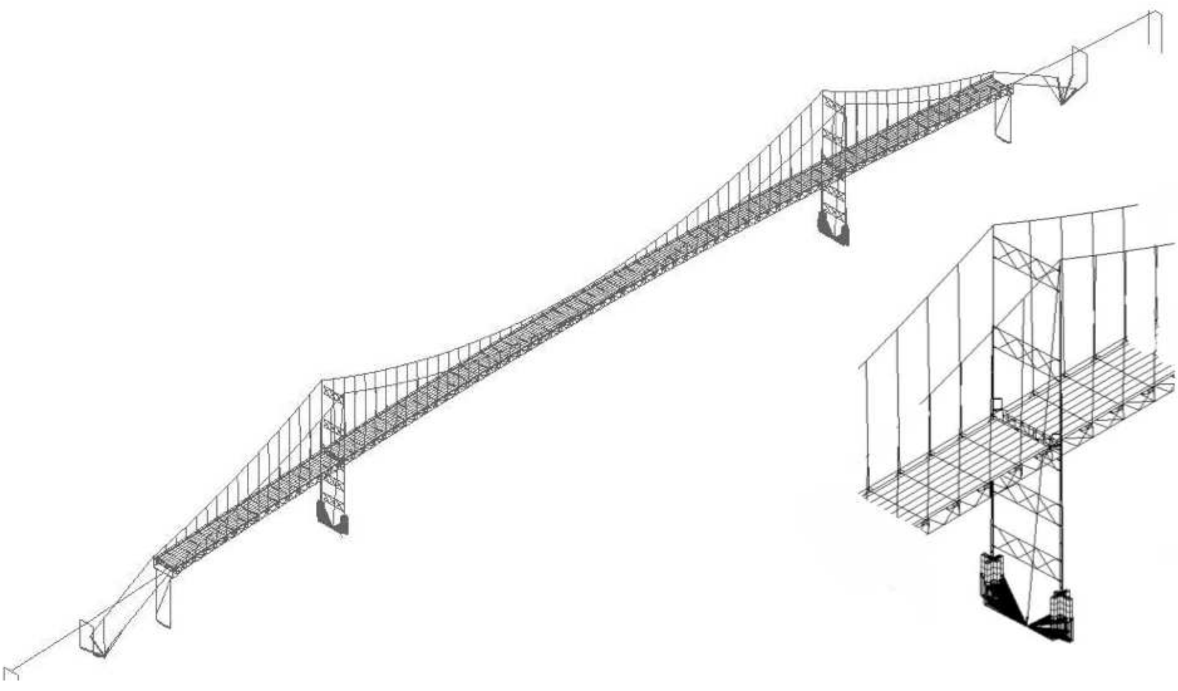

Figure 2. Finite element model of the Vincent Thomas Bridge.

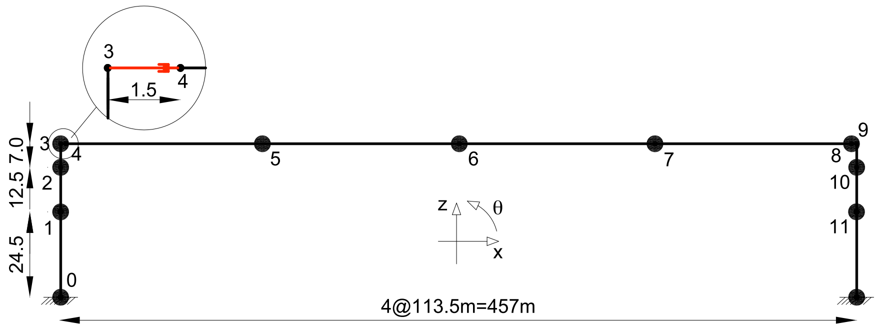

Figure 3. Bridge interpretative scheme with 12 elements (measurements in meters).

The application of the damage identification procedure does not require, in fact, the support of an FE model. The procedure requires, instead, a simplified interpretative scheme, as illustrated in the following subsection. The scheme is used for the discretization of the real structure in subcomponents (pylons, deck, and so on) and single elements, to allow the calculation of the normalized damage index for each element j, via $(2\text{-}10)_2$. The number and length of the elements that constitute the interpretative scheme is arbitrary. In addition, not every portion of the existing structure needs to be included in the interpretative scheme. In the following application, for instance, the main focus on damper performance verification justified the simplified interpretative scheme of Figure 3 to be limited to the bridge central span and the pylons. It must be noted that the interaction between all the structural components, and not only the ones represented in the simplified scheme, is accounted for in the response signals.

3.1. ***Vincent Thomas Bridge application: numerical data.*** The Vincent Thomas Bridge, located in the Los Angeles metropolitan area, is a cable-suspension bridge, 1849 m long, consisting of a main suspended span of approximately 457.5 m, two suspended side spans of 154 m each, ten spans in the San Pedro approach of approximately 560.6 m total length and ten spans in the Terminal Island approach of 522 m total length. The roadway width between curbs is typically 16 m and accommodates four lanes of traffic. The bridge construction was completed by the California Department of Transportation (Caltrans) in 1964. A substantial intervention of seismic upgrading was performed in 1980 and included, among others, the modification to the vertical cross frames, the lateral bracings near the bents, the cables restrainers, shear key abutment seats etc. In 1988 an additional seismic retrofit intervention included the stiffening of the bridge towers, the installation of structural fuses in the side spans and the installation of viscous dampers.

The dampers of interest for this research are located at the connection between pylons and deck, on both sides of the pylons (pylons to midspan and pylons to side-span). Other devices were not considered in this case study.

The finite element model of the bridge (Figure 2) consists of 3D elastic truss elements to represent the main suspension cables and suspender cables, 2D solid and shell elements to model the bridge deck, and beam elements to model the stiffening trusses and tower shafts. The viscous dampers are modeled by means of nonlinear spring elements with assigned stiffness and damping properties represented by a classic force-velocity relationship of the type $F = CV^a$. Here C and a represent the damping and velocity coefficients, respectively, while V is the velocity term.

	Frequency (Hz)			Coefficient c_i		
Case	Mode 1	Mode 2	Mode 3	Mode 1	Mode 2	Mode 3
D0	0.260	0.480	0.739	—	—	—
D30	0.274	0.477	0.746	1.000	0.116	0.176
D50	0.276	0.477	0.750	1.000	0.232	0.553

Table 1. Modal frequencies and coefficients of mode importance for bridge model.

Acceleration records were obtained from the numerical model of the bridge in three different configurations: bridge undamaged (case D0) and bridge with reduction of the performance characteristic of the dampers by 30% (case D30) and 50% (case D50). The degradation of the damper performance was simulated for the main span-tower dampers in terms of reduction of their damping coefficient with respect to the nominal values. The input excitation was provided through a white noise signal with frequencies between 0 and 60 Hz. The same signal was utilized for the bridge in undamaged and damaged condition.

Only the portion of the structure mostly affected by the dampers, specifically the pylons and the main span deck (see interpretative scheme of Figure 3), was considered in this phase. As indicated above, additional portions of the overall bridge can be added, like the complete height of the towers and the structure from the towers to the abutments, but the selected part of the bridge seemed appropriate for the goal of initial validation of the procedure. The dampers connecting the bridge towers and the main-span deck are also grouped, in the schematic of Figure 3, in two elements (element between node 3 and 4 and element between nodes 8 and 9). Each element represents a set of 4 dampers in the real structure. An higher level of analysis could represent each single damper by one specific element of the interpretative scheme.

The assessment of the mode shapes from the FE model response signals was obtained by use of the output-only response method proposed in [Peeters 2000], based on SSI-Cov. The output-only characteristic of the method is considered of paramount importance for the proposed application because the structure is treated as excited by unmeasurable input force and only output measurements (such as accelerations) are available. This condition closely represents the reality of a complex structure under a program of monitoring for structural health assessment purposes. For the SSI-Cov method the deterministic knowledge of the input is replaced by the assumption that the input is a realization of a stochastic process (white noise). An efficient construction of the stabilization diagram was achieved by computing the single value decomposition (SVD) of the covariance Toeplitz matrix only once. The natural frequencies for the first three modes and the coefficient c_i, as defined in (2-9), are reported in Table 1.

The normalized damage index Z_{ij}, for the 50% damage scenario, is reported in Figure 4 for the first three modes. For visualization purposes, the elements that represent the east pylon, the deck and the west pylon are projected on the same x axis. The damage indexes for the two energy dissipators, at the pylon to main-span location, are reported at the right end side of the diagram. In Figure 4, at the damper locations, the index Z_j exceeds the value of 2, indicating a degradation associated with these elements. Figure 5, left, shows the normalized damage index given in $(2\text{-}10)_2$ after the combination of the first

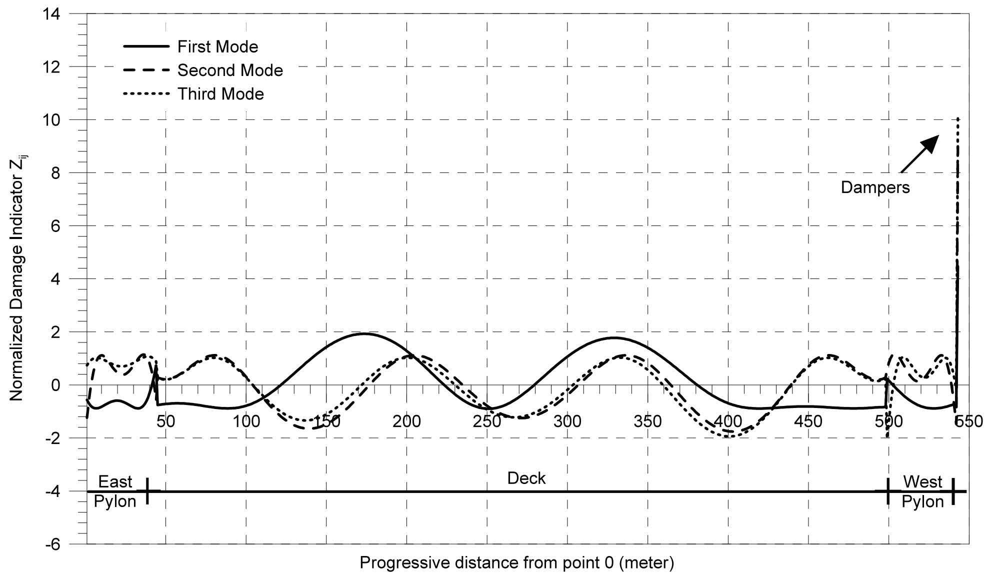

Figure 4. Damage 50%: normalized damage index Z_{ij} of the first three modes.

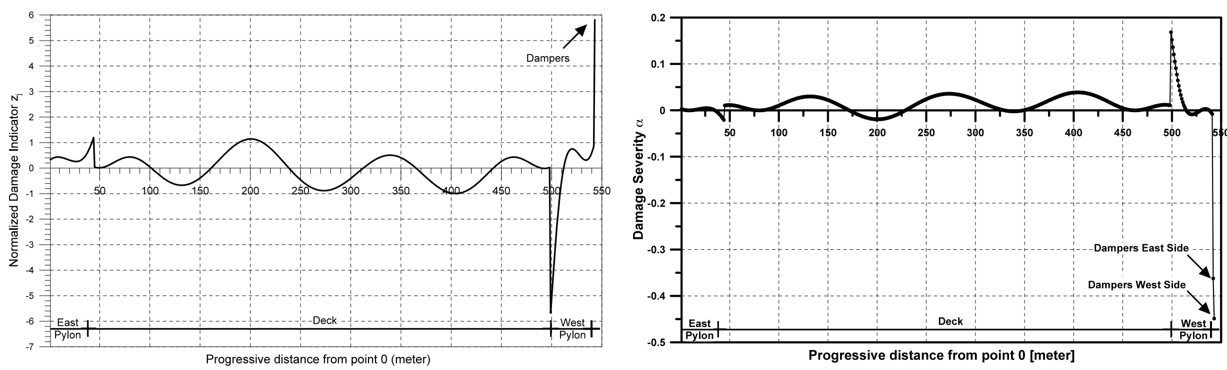

Figure 5. Damage 50%: normalized damage index Z_j (left) and damage severity α_j (right).

three modes. The severity index α_j, plotted in Figure 5, right, indicates a degradation level of $\sim 37\%$ for the dampers on the East side of the main span and of $\sim 45\%$ for the dampers on the West side.

3.2. ***Vincent Thomas Bridge application: experimental data.*** Ambient vibration data were collected on the bridge by the sensor network indicated in Figure 6. Only the East side of the bridge is presently monitored by 26 accelerometers. Data were recorded on different events dated April 2003, June 2006 and December 2006. The data set represents a unique opportunity for validation of the proposed approach. In fact, April 2003 and June 2006 data sets correspond to a bridge configuration with degraded dampers, as observed by on site investigations and post-removal laboratory tests. By December 2006, four dampers were removed from the bridge and replaced with new identical units. For these reasons, reverting the time sequence of events, the December 2006 data were used as undamaged configuration and the April 2003 to June 2006 data were used to verify the damper conditions.

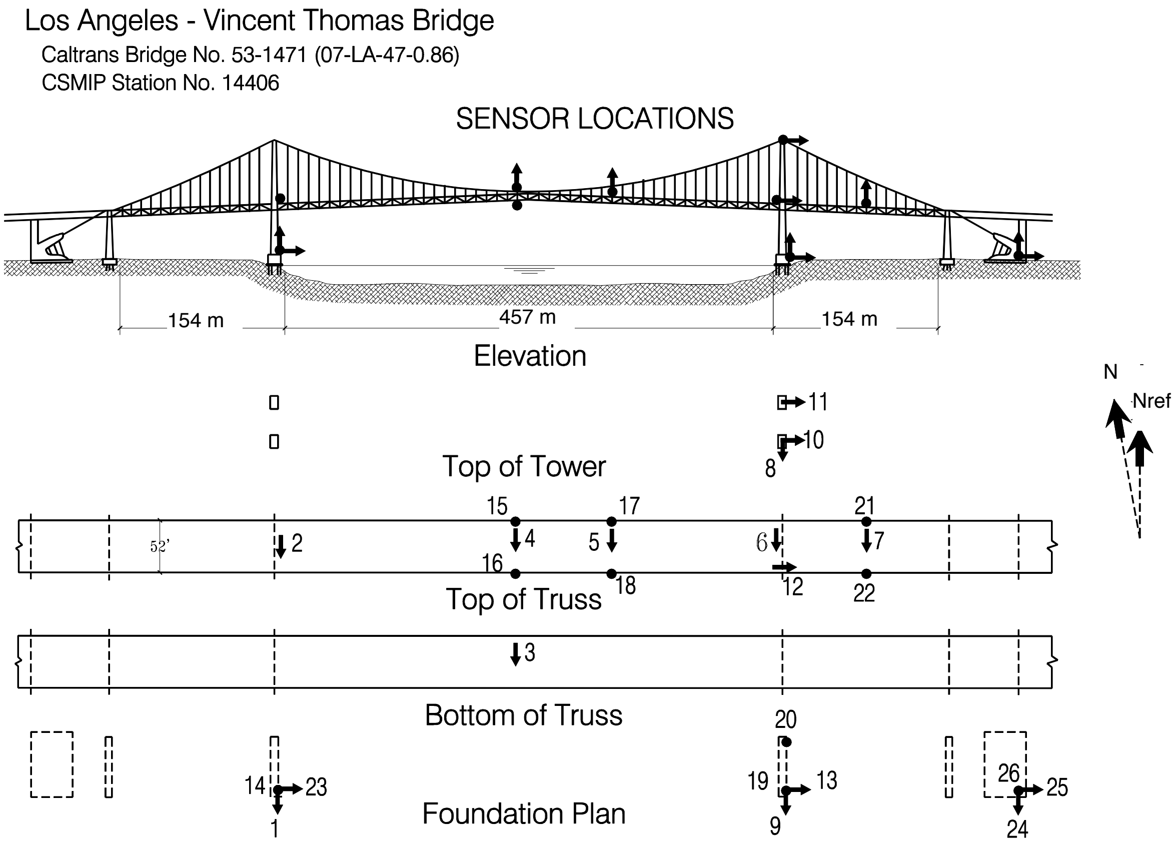

Figure 6. Sensor locations, from [Smyth et al. 2003].

A set of records from the Chino Hills earthquake (July 2008) were finally compared with the records of December 2006 in order to verify the damper characteristics, with the expectation to obtain a nondamaged scenario due to the early replacement during year 2006. As outlined in the paragraphs above, the recorded data were initially used to estimate mode shapes for the first three significant modes of the deck and pylons. Three acceleration time histories (Channels 15, 17 and 21) were used for the deck's mode shapes and three sensor readouts (Channels 13, 12 and 10) were used for the pylon's mode shapes. The natural frequencies for the first three modes and the coefficients of mode importance — see (2-9) — are reported in Table 2.

The interpretative scheme of the bridge under consideration is shown in Figure 7. The node selection reflects both the availability of sensor readouts (numbers in parenthesis) as well as the need of providing points of connection between elements (nodes 3, 4, 8) and boundary locations (node 6). After the assessment of the mode shape functions, each segment of the structure between nodes was further subdivided in a larger number of elements, each 1 m long, used for the computation of the damage indices. The damage detection algorithm was applied here only to the deck portion of the bridge and to the viscous damper elements. Pylons were not analyzed, in terms of damage evaluation, due to the limited number of sensors installed on them. Pylon mode shapes, however, were obtained in order to estimate the relative

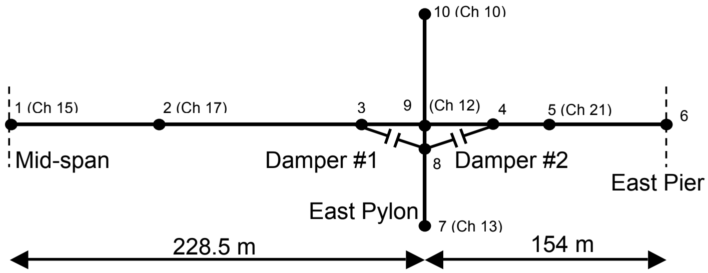

Figure 7. Interpretative scheme of the Vincent Thomas Bridge (measurements in meters).

displacements across the dampers. Figure 8 shows the damage index Z_j obtained as combination of the first three modal contributions. The estimate of the modes shapes was performed from acceleration data recorded on the bridge in December 2006 and April 2003 at the locations 1, 2, 9 and 5 corresponding to sensors in Channels 15, 17, 12 and 21, respectively (see Figure 7).

An interpolating function of the modes shapes was obtained in order to estimate the modal displacements at locations 3, 4 and 6 where sensors are not available. The mode shape of the pylon allowed the assessment of the relative modal displacement across the two sets of dampers (#1 and #2), located, for graphical representation, at the right side of Figure 8. The left part of the figure indicates damage in

	Frequency (Hz)			Coefficient c_i		
	Mode 1	Mode 2	Mode 3	Mode 1	Mode 2	Mode 3
Dec. 2006	0.25	0.39	0.46	—	—	—
Apr. 2003	0.22	0.37	0.46	1.0	0.40	0.30
June 2006	0.24	0.34	0.54	1.0	0.40	0.30
July 2008	0.32	0.43	0.62	1.0	0.30	0.70

Table 2. Modal frequencies and coefficients of mode importance for real structure.

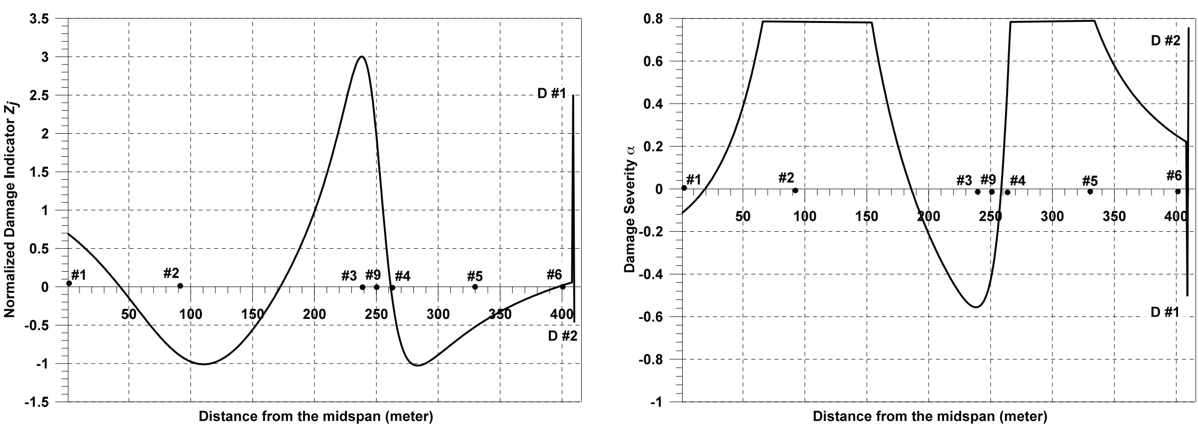

Figure 8. Data from December 2006 and April 2003: normalized damage index Z_j (left) and damage severity α_j (right).

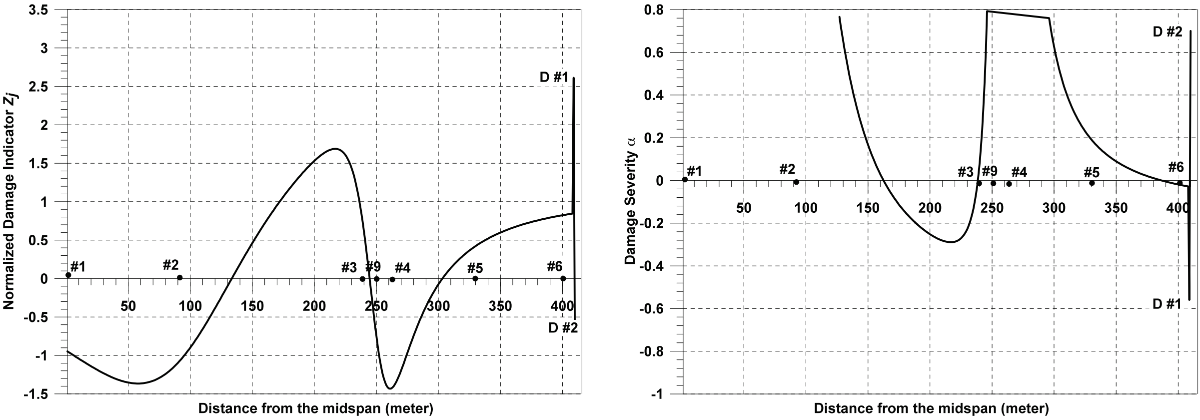

Figure 9. Data from December 2006 and June 2006: normalized damage index Z_j (left) and damage severity α_j (right).

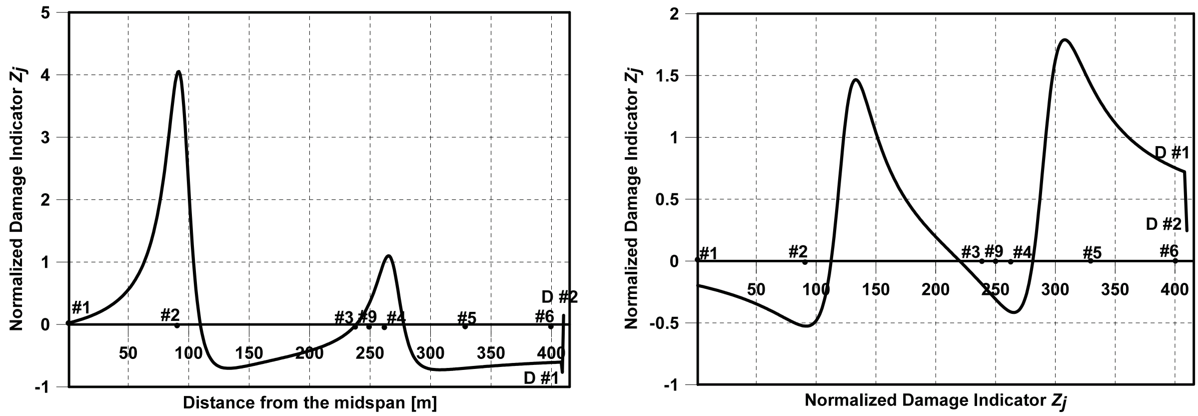

Figure 10. Data from December 2006 and July 2008: normalized damage index Z_j (left) and damage severity α_j (right).

the first damper set (#1) and for the deck elements between 220 to 250 m from the bridge midspan. For these elements the normalized damage index Z_j is, in fact, greater than 2. The severity of the damage, confirmed by the negative value of the coefficient α_j in Figure 8, right, is approximately 50% when compared with the undamaged configuration of the dampers. An additional analysis was performed using the data set obtained in June 2006 and using as reference configuration the December 2006 records. The results, presented in Figure 9, confirm the degradation of the damper performance for device #1 as well as the probable damage of deck elements in the region at 220–250 m from midspan. The last comparison, between bridge conditions in December 2006 and during the seismic event of July 2008 does not indicate any degradation of the dampers, as expected due to their replacement with new devices.

4. Conclusions

An existing structural health monitoring technique was adapted and improved in order to be used for bridge structures equipped with the use of viscous dampers. The procedure appears quite accurate for the detection of variations in the performance of the dissipation devices as well as in the remaining structural elements. One of the benefits of the procedure is the requirement of traditional sensors (accelerometers) not specifically installed in the proximity of the devices. The minimum number of installed sensors must however allow a reasonable assessment of the fundamental mode shapes of the bridge components (pylons, deck, and so on). The approach is presently under study for his potential application to bridges protected by common antiseismic devices such as elastomeric bearings and friction-based sliders.

Acknowledgements

The current research was supported by grants provided by the California Department of Transportation. The authors gratefully acknowledge the project manager, Dr. Charles Sikorsky, for the invaluable contribution to this project.

References

[Benzoni et al. 2007] G. Benzoni, C. Amaddeo, A. D. Cesare, and P. Palermo, “A damage identification procedure for bridge structures with energy dissipation devices”, technical report SRMD-2007/08, Department of Structural Engineering, University of California San Diego, La Jolla, CA, 2007.

[Housner et al. 1997] G. W. Housner, L. A. Bergman, T. K. Caughey, A. G. Chassiakos, R. O. Claus, S. F. Masri, R. E. Skelton, T. T. Soong, B. F. Spencer, and J. T. P. Yao, “J.T.P, "Structural control: past, present and future"”, *J. Eng. Mech.* (*ASCE*) **123**:9 (1997), 897–971.

[Peeters 2000] B. Peeters, *System identification and damage detection in civil engineering*, Ph.D. thesis, Department of Civil Engineering, Katholieke Universiteit Leuven, Louvain, Belgium, 2000, available at www.kuleuven.be/bwm/papers/peet00a.pdf.

[Smyth et al. 2003] A. W. Smyth, J. S. Pei, and S. F. Masri, “System identification of the Vincent Thomas suspension bridge using earthquake records”, *Earthquake Engin. Struct. Dyn.* **32** (2003), 339–367.

[Stubbs et al. 1992] N. Stubbs, J.-T. Kim, and K. Topole, “An efficient and robust algorithm for damage localization in offshore platforms”, pp. 543–546 in *Proc. ASCE 10th Structures Congress* (San Antonio, TX), ASCE, New York, 1992.

Received 16 Aug 2010. Accepted 30 Sep 2010.

GIANMARIO BENZONI: benzoni@ucsd.edu
University of California San Diego, Department of Structural Engineering, 9500 Gilman Drive, Mail Code 0085, La Jolla, CA 92093, United States

CARMEN AMADDEO: camaddeo@gmail.com
Università Mediterranea di Reggio Calabria, Loc. Feo di Vito, I-89100 Reggio Calabria, Italy

SEISMIC ISOLATION AND PROTECTIVE SYSTEMS

http://pjm.math.berkeley.edu/siaps/

See inside back cover or http://www.jomms.org for submission guidelines.

SIAPS (ISSN 2150–7902) is published in electronic form only. The subscription price for 2010 is US $150/year. Subscriptions, requests for back issues, and changes of address should be sent to Mathematical Sciences Publishers, Department of Mathematics, University of California, Berkeley, CA 94720–3840.

SIAPS peer-review and production is managed by EditFLOW™ from Mathematical Sciences Publishers.

PUBLISHED BY
mathematical sciences publishers
http://www.mathscipub.org
A NON-PROFIT CORPORATION
Typeset in LaTeX

Seismic Isolation and Protection Systems vol 1, no 1, 2010

2150-7902(2010)1:1;1-G